Quantum dot-organic molecule conjugates as hosts for photogenerated spin qubit pairs

Autumn Y. Lee,[1,†] Troy A. Colleran,[1,†] Amisha Jain,[1,†] Jens Niklas,[2] Brandon K. Rugg,[3] Tomoyasu Mani,[4] Oleg G. Poluektov,[2] Jacob H. Olshansky[1,*]

[1]Department of Chemistry, Amherst College, Amherst, Massachusetts 01002, United States
[2]Chemical Sciences and Engineering Division, Argonne National Laboratory, Lemont, Illinois 60439, United States
[3]Chemistry and Nanosciences Center, National Renewable Energy Laboratory, Golden, Colorado 80401, United States
[4]Department of Chemistry, University of Connecticut, Storrs, Connecticut 06269-3060, United States

KEYWORDS photogenerated spin qubit pairs, quantum information science, zinc oxide quantum dots, time-resolved EPR

ABSTRACT: The inherent spin polarization present in photogenerated spin-correlated radical pairs make them promising candidates for quantum computing and quantum sensing applications. The spin states of these systems can be probed and manipulated with microwave pulses using electron paramagnetic resonance spectrometers. However, to date, there are no reports on magnetic resonance-based spin measurements of photogenerated spin correlated-radical pairs hosted on quantum dots. In the current work, we prepare dye molecule – inorganic quantum dot conjugates and show that they can produce photogenerated spin-polarized states. The dye molecule, D131, is chosen for its ability to undergo efficient charge separation and the nanoparticle materials, ZnO quantum dots, are chosen for their promising spin properties. Transient and steady state optical spectroscopy performed on ZnO quantum dot – D131 conjugates shows that reversible photogenerated charge separation is occurring. Transient and pulsed electron paramagnetic resonance experiments are then performed on the photogenerated radical pair which demonstrate that 1) the radical pair is polarized at moderate temperatures and well modelled by existing theories and 2) the spin states can be accessed and manipulated with microwave pulses. This work opens the door to a new class of promising qubit materials that can be photogenerated in polarized states and hosted by highly tailorable inorganic nanoparticles.

Photogenerated spin-correlated radical pairs (SCRP) have drawn interest for their potential applications in quantum information science (QIS).[1,2] They are particularly attractive as qubits since they are prepared in well-defined, highly polarized (non-Boltzmann populated) spin states without requiring millikelvin cooling. More recently they have been referred to as spin qubit pairs (SQP). These SQPs can be generated when a singlet state is photoexcited and allowed to undergo (rapid) charge separation. The electron spins that compose the resulting radical anion and radical cation represent a qubit pair with four accessible states, but initially populated in only two of those states. Spin manipulations of SQPs can be readily implemented using microwave pulse sequences in electron paramagnetic resonance (EPR) spectrometers. Early studies on SCRPs were performed on molecules in micelles,[3,4] photosynthetic reaction centers,[5–7] and surface states in TiO_2.[8,9] More recent work on SQPs have been focused on a variety of synthetic organic donor-acceptor complexes,[2,10–12] and DNA.[13–16] Notably, the utility of SQPs for quantum operations has been demonstrated in these materials, and crucially relies upon spectrally separable spins.[16–20] In the current work, we show that colloidal quantum dots can also serve as promising hosts for SQPs, and provide some advantages over the well-studied all-organic systems.

Colloidal quantum dots (QDs) are semiconducting nanoparticles that exhibit quantum confinement effects of photogenerated charges. They offer a flexible platform for studying SQPs owing to both their size tunable electronic and spin properties as well as their surface functionality. QDs can be surface functionalized with charge accepting or donating molecular species to produce the donor-acceptor dyads necessary for SQPs.[21–27] Furthermore, the spin states in QDs can have *g*-values far from the 1.99-2.01 range common to organic molecules.[28–33] This enables more straightforward spin specific addressability than can be achieved with all-organic SQPs,[14] thus satisfying a key requirement of functional qubit systems.[34] It should be noted that significantly distinct *g* values will be difficult to simultaneously probe due to limitations in EPR resonator bandwidths. Nevertheless, directly probing and manipulating SQPs in QDs *via* EPR is only possible if they can host spin states with long (>>100 ns) decoherence times.

Electron spin states have been probed with a variety of techniques for both zinc oxide QDs and cadmium chalcogenide (CdE) QDs, revealing that ZnO QDs have

dramatically elongated spin lifetimes as compared to CdE QDs.[31,32,35–38] Therefore, although the SCRP model has been employed to understand behavior of CdE QD – molecular dyads,[39–42] rapid spin relaxation has precluded direct measurements and spin manipulations *via* EPR of these systems. For example, prior work has demonstrated spin polarization of an appended molecular radical in such systems, but the spin state localized on the CdE QDs was not observed by EPR, most likely due to rapid relaxation.[39] Electron spins on ZnO QDs, however, have been probed *via* EPR and exhibit T_1 relaxation times on the order of a microsecond and T_2 relaxation times of 25-50 ns at room temperature.[35,36] These spin states have been prepared by photochemically reducing ZnO QDs to produce stably trapped delocalized electrons in the conduction band.[43,44] The *g* value of these electrons is size tunable, ranging from 1.96 to 1.97 depending on the QD size.[28–30] This is a useful range of *g* values since they are distinct enough to produce resonances separable from organic radicals, but close enough in frequency to be simultaneously manipulated with a moderate bandwidth resonator. Nevertheless, measurements done thus far on these spin states are akin to probing stable radicals, as they are Boltzmann-populated with minimal spin polarization at moderate temperatures.

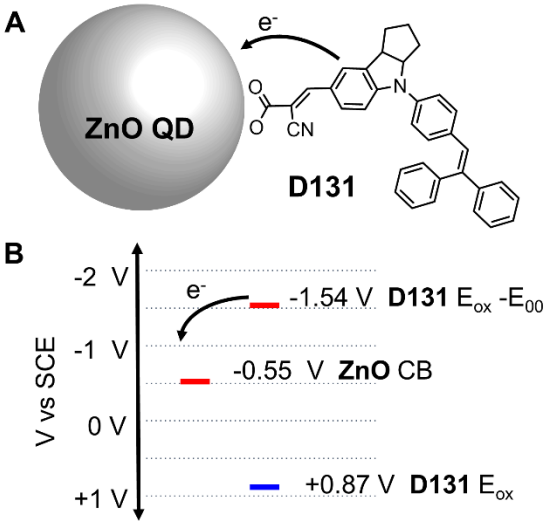

Figure 1. ZnO quantum dot – D131 dye molecule (A) cartoon and (B) energetics.

The current work takes advantage of these stable spin states in ZnO QDs to prepare QD hosted photogenerated SQPs. To achieve this, we functionalize the surface of ZnO QDs with dye molecules so that when the dye-NP conjugate is photoexcited, an electron is transferred to the conduction band of the ZnO QDs. The resulting SQP is long-lived such that pulse EPR experiments are feasible. We demonstrate that delocalized spin states in QDs can be prepared with well-defined (polarized) populations, and manipulated coherently with microwave pulses. To our knowledge, this is the first report of the direct EPR measurement of a photogenerated SQP with a reduced QD as one of the components of the charge-separated radical pair.

Motivated by dye-sensitized solar cells (DSSCs) literature, we prepared organic dye – ZnO QD conjugates that upon photoexcitation produce long-lived charge-separated states.[24–27,45–48] We chose the indoline dye molecule D131 (Figure 1A) since it can be easily obtained, contains a carboxylic acid group for binding to QD surfaces, and has successfully been used in ZnO-based DSSCs that require efficient charge separation with long charge separation lifetimes. The ZnO QDs were synthesized based on a prior literature.[26] QD diameters and extinction coefficients were determined using UV-Vis absorption spectroscopy and previously determined experimentally based sizing curves (see SI).[49,50] The energetics of the D131 – ZnO QD system have previously been determined experimentally: the oxidation potential, E_{ox}, *via* electrochemistry, and the excited state energy, E_{00}, *via* optical absorption.[47] These energetics are shown schematically in Figure 1B, and predict that photoexcited D131 will transfer an electron to the conduction band of ZnO to produce the radical pair of $D131^{\bullet+}$ and $ZnO^{\bullet-}$, which later recombines to the neutral ground state of D131 and ZnO.

We perform a series of steady state and transient optical experiments to ensure that the radical pair of $D131^{\bullet+}$ and $ZnO^{\bullet-}$ is indeed forming (Figure 2). Steady state measurements show that the absorption of D131 shifts and the fluorescence is significantly quenched upon addition of ZnO QDs. These observations suggest that D131 binds to ZnO and that photoexcited charge transfer occurs. An adsorption isotherm was additionally performed and fit well to the Langmuir model, revealing a maximum dye adsorption per QD of ~44 (see SI, Figure S3). Femtosecond transient absorption spectroscopy at room temperature on the D131-ZnO QDs reveals the decay of excited state D131* (feature at ~620 nm)[51] and the formation of radical cation $D131^{\bullet+}$ (feature at ~520 nm)[51] in ~10-30 ps, indicative of rapid charge separation (Figure 2C). The charge separated lifetime is also substantially longer than 7 ns, the time window of the measurement. As a whole, optical spectroscopy demonstrates the presence of a D131 – ZnO QD interaction as well as production of the $D131^{\bullet+}$ – $ZnO^{\bullet-}$ radical pair.

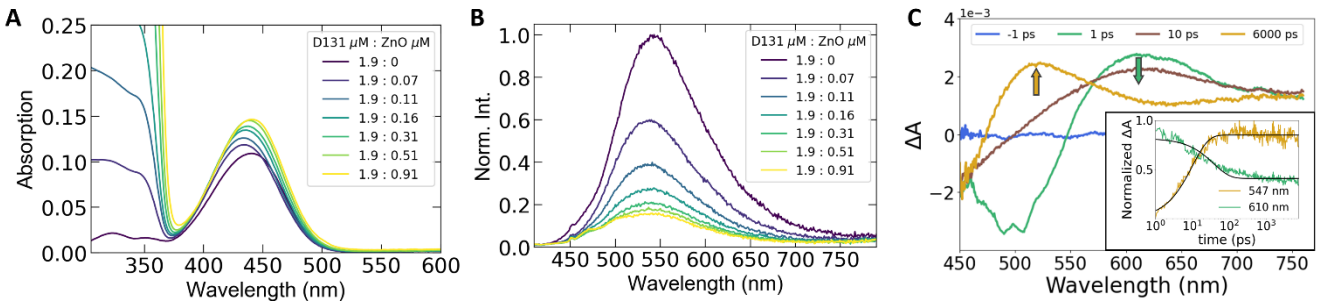

Figure 2. Steady state and transient optical spectroscopy. A) Absorption spectra of D131 with varying concentrations of ZnO QDs in tetrahydrofuran. B) Fluorescence spectra of D131, excited at 400 nm, with varying concentrations of ZnO QDs. C) Femtosecond transient absorption spectroscopy for D131 -ZnO QD conjugates in toluene. All measurements were performed at room temperature.

With a basic understanding of the dye – QD interactions and charge transfer kinetics at ambient temperature, we utilize time-resolved EPR spectroscopy to understand the spin dynamics. We analyze the spin states within the framework of the spin-correlated radical pair (SCRP) model (Figure 3).[4,52–56] In this model, the radicals are spatially separated such that the difference in hyperfine splitting and g values of the individual radicals is on the same order of magnitude as the distance-dependent exchange coupling (J) and dipolar coupling (D). This allows coherent spin evolution to occur, mixing the singlet and triplet states of the radical pair.

In a magnetic field, Zeeman splitting pushes the T_+ and T_- ($m_s = \pm 1$) triplet states of the weakly interacting radical pair to energies well above and below the photogenerated singlet (S) state, respectively. The initially populated S state will selectively mix with the T_0 ($m_s = 0$) state to produce two states with combined singlet and triplet character. This results in a well-defined four-state quantum system with all population in the two $m_s = 0$ states (Figure 3A).

These photogenerated SQPs can be probed with EPR since transitions within the triplet manifold are allowed. Transient EPR spectra, collected after laser excitation, are predicted to exhibit four transitions from the two occupied $m_s = 0$ states to initially unpopulated T_+ and T_- states. The resulting transient EPR spectra of weakly-coupled SQPs therefore consist of two emissive (e) and two absorptive (a) transitions that are centered at the g values of the two radical species (g_A and g_B). The exact energies of these four transitions for a single orientation of the radical pair with respect to the external magnetic field (denoted by angle θ) can be expressed in terms of two parameters, Δ and Ω (see Figure 3C) as (assuming axially symmetric dipolar interactions):[52,55,57]

$$\Delta = 2(J - d) \tag{1}$$

$$\Omega = \sqrt{\left(J + \frac{d}{2}\right)^2 + \frac{\mu_B^2 B^2}{4}(g_A - g_B)^2} \tag{2}$$

where

$$d = \frac{1}{3}D(3\cos^2\theta - 1) \tag{3}$$

When both radicals are organic species, these spectral signatures often overlap since the g values are all very close to 2.00. However, our photogenerated radical pair consisting of $D131^{\bullet+}$ and $ZnO^{\bullet-}$ should exhibit separable features for $D131^{\bullet+}$ at around g ~2.003 (see SI for calculations) and $ZnO^{\bullet-}$ at ~1.96.[28–30] We therefore expect to see an *e, a, e, a* polarization pattern from low to high magnetic field or from high to low frequency, such as in Figure 3C. With an understanding of the origins and expectations for our SQP EPR spectra, we turn to experimental data for the D131-ZnO QD conjugates.

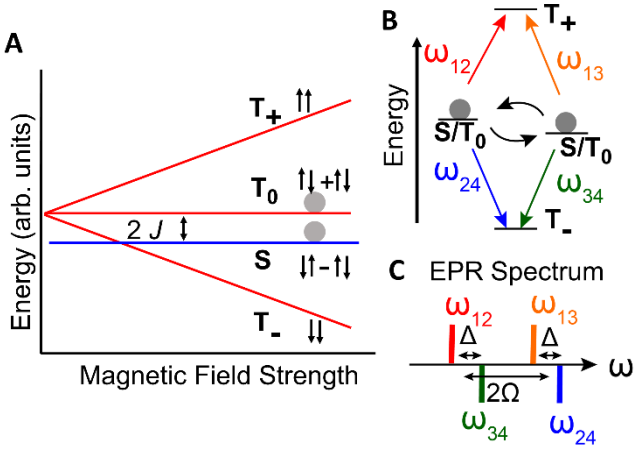

Figure 3. Photogenerated spin-correlated radical pair. (A) Energetics of singlet and triplet states in magnetic field (not to scale). (B) Mixing between $m_s = 0$ levels gives rise to two absorptive (red and orange) and two emissive (blue and green) transitions. (C) Predicted EPR spectral features.

Transient continuous wave EPR (TR-EPR) and pulse EPR on D131-ZnO QD conjugates suspended in toluene and photoexcited with a 450 nm laser are presented in Figure 4. Measurements were performed at 100 K on frozen solutions of (~11 μM) 5.8 nm diameter ZnO QDs with ~9 D131 molecules per QD (see SI for details). In TR-EPR experiments, samples are exposed to weak continuous resonant frequency microwave irradiation at a given magnetic field, and microwave absorption or emission is transiently recorded (see Figure

4A).[55] Figure 4B shows the field-dependence of this response averaged 600-1200 ns after visible laser excitation (black line). The transient EPR spectrum shows the expected *e, a, e, a* pattern. Since both radical species have highly isotropic *g* tensors, *g* anisotropy can be neglected at X-band, and Equations 1, 2, and 3 are used to simulate the experimental spectra. Computed spectra are generated for all possible orientations of the radical pair with respect to the external magnetic field (by varying θ) and summed to give the predicted spectrum (red dashed line).

There is good correspondence between the data and a model that employed a *g* value of 1.964 for $ZnO^{\bullet-}$, a near zero value for *J*, and a value for the dipolar coupling consistent with a radical pair separation of $r \geq 3$ nm (based on $D = -2785\ mT\ Å^{-3}/r^3$).[13] This separation is consistent with what we may predict for a 5.8 nm diameter ZnO QD with a dye molecule on the surface. However, simulations with multiple *D* values (SI, Figure S6) show that any distance greater than 3 nm is appropriate for simulating the experimental data. We do note deviations between the experiment and simulations near the D131 spectral signature. We attribute this to the highly anisotropic hyperfine coupling associated with the central nitrogen of D131 (see SI, Figure S4). Since the hyperfine interaction is not clearly resolved at X-band, and accurately modelling hyperfine anisotropy is a well-documented challenge in radical pair simulations, we have not explicitly included any hyperfine interactions but only treated all hyperfine interactions as isotropic broadening (see SI for details).

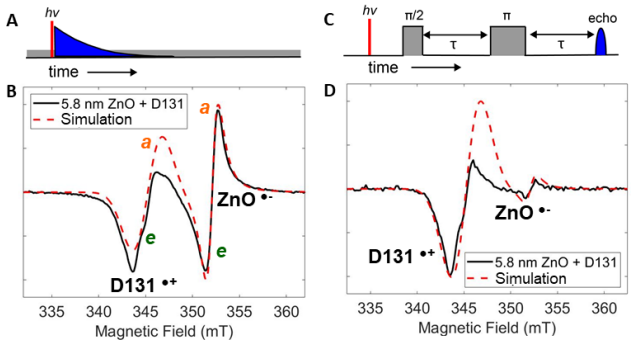

Figure 4. Time-resolved EPR data for ZnO QD – D131 conjugate in frozen toluene solutions. A) Schematic of transient continuous wave EPR (TR-EPR) experiment. B) TR-EPR (black) spectrum and (red dashed) simulation. C) Schematic of pulse EPR experiment. D) Field swept 2-pulse echo detected spectrum (black) and (red dashed) simulation. Emissive (*e*) and absorptive (*a*) features are labelled.

The TR-EPR data and associated theoretical modelling suggests that the $D131^{\bullet+}$ – $ZnO^{\bullet-}$ SQP is indeed photogenerated and possesses both the expected polarization and approximate geometry for the dye-QD system we have described. Furthermore, the spin pair is polarized at the moderate temperature of 100 K, thus highlighting the potential of this method. In separate experiments, we additionally found that spin polarized signals could be obtained at room temperature, albeit with lower signal to noise ratio (see SI, Figure S7).

In order to utilize this SQP as a qubit pair, we need to demonstrate that the spin pair can be manipulated with microwave pulses. A two-pulse Hahn echo EPR experiment was performed on the spin system after laser excitation (Figure 4C) for a series of magnetic field values. Notably, the field-swept echo response (Figure 4D) again shows the expected *e, a, e, a* polarization pattern. The resonances associated with $ZnO^{\bullet-}$ are significantly weaker than those belonging to $D131^{\bullet+}$. This is a result of enhanced T_2 spin relaxation on the ZnO QD. Nevertheless, the presence of a spin echo for both components of the qubit pair suggests that spin manipulation such as quantum gate operations can be performed.[18] Future work may employ deuterated solvents, removal of Zn^{67} (the only magnetic isotope: I=5/2, abundance 4.1%), and lower temperatures to extend spin coherence times.[36]

In conclusion, we have expanded the scope of materials that show promise for QIS applications. Specifically, we investigate photogenerated spin qubit pairs which offer inherent spin polarization at room temperature, a desirable trait for moving beyond cryo-cooled qubits. Prior to this work, the spin states of these photogenerated spin qubit pairs had primarily been investigated when localized on organic systems. Here, we demonstrate that a conjugate composed of a dye molecule (D131) and an inorganic nanoparticle (ZnO QDs) can host photogenerated spin qubit pairs. Furthermore, the polarized spin states can be probed and manipulated with pulse EPR techniques. We hope that this report inspires additional investigation of photogenerated spin states in the highly tunable and promising system of quantum dot-molecule conjugates.

ASSOCIATED CONTENT

Supporting Information. Experimental methods for synthesis of ZnO QDs and preparation of QD – molecule conjugates. D131 optical extinction data and binding isotherms. Instrumentation details for optical studies and EPR experiments. Details on EPR simulations including DFT calculations on the D131 radical cation. Continuous wave EPR data and associated fits. Room temperature TR-EPR data. This material is available free of charge via the Internet at http://pubs.acs.org.

AUTHOR INFORMATION

Corresponding Author

* E-mail: jolshansky@amherst.edu

Author Contributions

† A.Y.L., T.A.C., and A.J. contributed equally to this work.

ACKNOWLEDGMENT

This work is supported by the National Science Foundation under grant no. CHE-2154372 and grant no. CHE-2144787. Time-resolved EPR work was supported by the U.S. Department of Energy, Office of Science, Office of Basic Energy Sciences, Division of Chemical Sciences, Geosciences, and Biosciences,

through Argonne National Laboratory and the National Renewable Energy Laboratory under Contract Nos. DE-AC02-06CH11357 and DE-AC36-08GO28308, respectively. This work was authored in part by Alliance for Sustainable Energy, LLC, the manager and operator of the National Renewable Energy Laboratory. The views expressed in the article do not necessarily represent the views of the DOE or the US government. The US government retains and the publisher, by accepting the article for publication, acknowledges that the US government retains a nonexclusive, paid-up, irrevocable, worldwide license to publish or reproduce the published form of this work, or allow others to do so, for US government purposes.

REFERENCES

(1) Mani, T. Molecular Qubits Based on Photogenerated Spin-Correlated Radical Pairs for Quantum Sensing. *Chem. Phys. Rev.* **2022**, *3* (2), 021301. https://doi.org/10.1063/5.0084072.

(2) Harvey, S. M.; Wasielewski, M. R. Photogenerated Spin-Correlated Radical Pairs: From Photosynthetic Energy Transduction to Quantum Information Science. *J. Am. Chem. Soc.* **2021**, *143* (38), 15508–15529. https://doi.org/10.1021/jacs.1c07706.

(3) Tarasov, V. F.; Yashiro, H.; Maeda, K.; Azumi, T.; Shkrob, I. A. Spin-Correlated Radical Pairs in Micellar Systems: Mechanism of CIDEP and the Micelle Size Dependence. *Chem. Phys.* **1996**, *212* (2), 353–361. https://doi.org/10.1016/S0301-0104(96)00145-0.

(4) Closs, G. L.; Forbes, M. D. E.; Norris, J. R. Spin-Polarized Electron Paramagnetic Resonance Spectra of Radical Pairs in Micelles: Observation of Electron Spin-Spin Interactions. *J. Phys. Chem.* **1987**, *91* (13), 3592–3599. https://doi.org/10.1021/j100297a026.

(5) Hoff, A. J. Magnetic Resonance of Bacterial Photosynthetic Reaction Centers. In *Photosynthetic Reaction Center*; Deisenhofer, J., Norris, J. R., Eds.; Academic Press: San Diego, 1993; pp 331–386. https://doi.org/10.1016/B978-0-12-208662-5.50017-7.

(6) DiMagno, T. J.; Norris, J. R. Initial Electron Transfer Events in Photosynthetic Bacteria. In *Photosynthetic Reaction Center*; Academic Press, 2013; pp 105–132.

(7) Snyder, S. W.; Thurnauer, M. C. Electron Spin Polarization in Photosynthetic Reaction Centers. In *Photosynthetic Reaction Center*; Deisenhofer, J., Norris, J. R., Eds.; Academic Press: San Diego, 1993; pp 285–330. https://doi.org/10.1016/B978-0-12-208662-5.50016-5.

(8) Dubinski, A. A.; Perekhodtsev, G. D.; Poluektov, O. G.; Rajh, T.; Thurnauer, M. C. Analytical Treatment of EPR Spectra of Weakly Coupled Spin-Correlated Radical Pairs in Disordered Solids: Application to the Charge-Separated State in TiO_2 Nanoparticles. *J. Phys. Chem. B* **2002**, *106* (5), 938–944. https://doi.org/10.1021/jp013276h.

(9) Rajh, T.; Poluektov, O.; Dubinski, A. A.; Wiederrecht, G.; Thurnauer, M. C.; Trifunac, A. D. Spin Polarization Mechanisms in Early Stages of Photoinduced Charge Separation in Surface-Modified TiO2 Nanoparticles. *Chem. Phys. Lett.* **2001**, *344* (1), 31–39. https://doi.org/10.1016/S0009-2614(01)00733-3.

(10) Hasharoni, K.; Levanon, H.; Greenfield, S. R.; Gosztola, D. J.; Svec, W. A.; Wasielewski, M. R. Mimicry of the Radical Pair and Triplet States in Photosynthetic Reaction Centers with a Synthetic Model. *J. Am. Chem. Soc.* **1995**, *117* (30), 8055–8056. https://doi.org/10.1021/ja00135a040.

(11) Wasielewski, M. R. Energy, Charge, and Spin Transport in Molecules and Self-Assembled Nanostructures Inspired by Photosynthesis. *J. Org. Chem.* **2006**, *71* (14), 5051–5066. https://doi.org/10.1021/jo060225d.

(12) Carbonera, D.; Di Valentin, M.; Corvaja, C.; Agostini, G.; Giacometti, G.; Liddell, P. A.; Kuciauskas, D.; Moore, A. L.; Moore, T. A.; Gust, D. EPR Investigation of Photoinduced Radical Pair Formation and Decay to a Triplet State in a Carotene−Porphyrin−Fullerene Triad. *J. Am. Chem. Soc.* **1998**, *120* (18), 4398–4405. https://doi.org/10.1021/ja9712074.

(13) Olshansky, J. H.; Krzyaniak, M. D.; Young, R. M.; Wasielewski, M. R. Photogenerated Spin-Entangled Qubit (Radical) Pairs in DNA Hairpins: Observation of Spin Delocalization and Coherence. *J. Am. Chem. Soc.* **2019**, *141* (5), 2152–2160. https://doi.org/10.1021/jacs.8b13155.

(14) Olshansky, J. H.; Zhang, J.; Krzyaniak, M. D.; Lorenzo, E. R.; Wasielewski, M. R. Selectively Addressable Photogenerated Spin Qubit Pairs in DNA Hairpins. *J. Am. Chem. Soc.* **2020**, *142* (7), 3346–3350. https://doi.org/10.1021/jacs.9b13398.

(15) Lorenzo, E. R.; Olshansky, J. H.; Abia, D. S. D.; Krzyaniak, M. D.; Young, R. M.; Wasielewski, M. R. Interaction of Photogenerated Spin Qubit Pairs with a Third Electron Spin in DNA Hairpins. *J. Am. Chem. Soc.* **2021**, *143* (12), 4625–4632. https://doi.org/10.1021/jacs.0c12645.

(16) Carmieli, R.; Thazhathveetil, A. K.; Lewis, F. D.; Wasielewski, M. R. Photoselective DNA Hairpin Spin Switches. *J. Am. Chem. Soc.* **2013**, *135* (30), 10970–10973. https://doi.org/10.1021/ja4055405.

(17) Rugg, B. K.; Krzyaniak, M. D.; Phelan, B. T.; Ratner, M. A.; Young, R. M.; Wasielewski, M. R. Photodriven Quantum Teleportation of an Electron Spin State in a Covalent Donor–Acceptor–Radical System. *Nat. Chem.* **2019**, *11* (11), 981–986. https://doi.org/10.1038/s41557-019-0332-8.

(18) Nelson, J. N.; Zhang, J.; Zhou, J.; Rugg, B. K.; Krzyaniak, M. D.; Wasielewski, M. R. CNOT Gate Operation on a Photogenerated Molecular Electron Spin-Qubit Pair. *J. Chem. Phys.* **2020**, *152* (1), 014503. https://doi.org/10.1063/1.5128132.

(19) Kobr, L.; Gardner, D. M.; Smeigh, A. L.; Dyar, S. M.; Karlen, S. D.; Carmieli, R.; Wasielewski, M. R. Fast Photodriven Electron Spin Coherence Transfer: A Quantum Gate Based on a Spin Exchange J-Jump. *J. Am. Chem. Soc.* **2012**, *134* (30), 12430–12433. https://doi.org/10.1021/ja305650x.

(20) Miura, T.; Wasielewski, M. R. Manipulating Photogenerated Radical Ion Pair Lifetimes in Wirelike Molecules Using Microwave Pulses: Molecular Spintronic Gates.

J. Am. Chem. Soc. **2011**, *133* (9), 2844–2847. https://doi.org/10.1021/ja110789q.

(21) Harris, R. D.; Bettis Homan, S.; Kodaimati, M.; He, C.; Nepomnyashchii, A. B.; Swenson, N. K.; Lian, S.; Calzada, R.; Weiss, E. A. Electronic Processes within Quantum Dot-Molecule Complexes. *Chem. Rev.* **2016**, *116* (21), 12865–12919. https://doi.org/10.1021/acs.chemrev.6b00102.

(22) Irgen-Gioro, S.; Yang, M.; Padgaonkar, S.; Chang, W. J.; Zhang, Z.; Nagasing, B.; Jiang, Y.; Weiss, E. A. Charge and Energy Transfer in the Context of Colloidal Nanocrystals. *Chem. Phys. Rev.* **2020**, *1* (1), 011305. https://doi.org/10.1063/5.0033263.

(23) Knowles, K. E.; Peterson, M. D.; McPhail, M. R.; Weiss, E. A. Exciton Dissociation within Quantum Dot–Organic Complexes: Mechanisms, Use as a Probe of Interfacial Structure, and Applications. *J. Phys. Chem. C* **2013**, *117* (20), 10229–10243. https://doi.org/10.1021/jp400699h.

(24) Huss, A. S.; Rossini, J. E.; Ceckanowicz, D. J.; Bohnsack, J. N.; Mann, K. R.; Gladfelter, W. L.; Blank, D. A. Photoinitiated Electron Transfer Dynamics of a Terthiophene Carboxylate on Monodispersed Zinc Oxide Nanocrystals. *J. Phys. Chem. C* **2011**, *115* (1), 2–10. https://doi.org/10.1021/jp108028d.

(25) Huss, A. S.; Bierbaum, A.; Chitta, R.; Ceckanowicz, D. J.; Mann, K. R.; Gladfelter, W. L.; Blank, D. A. Tuning Electron Transfer Rates via Systematic Shifts in the Acceptor State Density Using Size-Selected ZnO Colloids. *J. Am. Chem. Soc.* **2010**, *132* (40), 13963–13965. https://doi.org/10.1021/ja104482t.

(26) Swedin, R.; Badgurjar, D.; Healy, A.; Harkins, R.; Oehrlein, A.; Greenlund, L.; Alshebber, M.; Ripp, N.; Anderson, N. T.; Honzay, B. R.; Pappenfus, T. M.; Janzen, D. E.; Blank, D. A.; Gladfelter, W. L. Excited State Electron Transfer from Donor−π System–Acceptor Dyes to ZnO Nanocrystals. *J. Phys. Chem. C* **2020**, *124* (28), 15565–15573. https://doi.org/10.1021/acs.jpcc.0c03828.

(27) Vatassery, R.; Hinke, J. A.; Sanchez-Diaz, A.; Hue, R.; Mann, K. R.; Blank, D. A.; Gladfelter, W. L. Excited-State Quenching Mechanism of a Terthiophene Acid Dye Bound to Monodisperse CdS Nanocrystals: Electron Transfer versus Concentration Quenching. *J. Phys. Chem. C* **2013**, *117* (20), 10708–10715. https://doi.org/10.1021/jp312272p.

(28) Whitaker, K. M.; Ochsenbein, S. T.; Polinger, V. Z.; Gamelin, D. R. Electron Confinement Effects in the EPR Spectra of Colloidal N-Type ZnO Quantum Dots. *J. Phys. Chem. C* **2008**, *112* (37), 14331–14335. https://doi.org/10.1021/jp804763y.

(29) Kim, H. H.; Lee, H.; Kang, J. K.; Choi, W. K. Photoluminescence and Electron Paramagnetic Resonance Spectroscopy for Revealing Visible Emission of ZnO Quantum Dots. *Ann. Phys.* **2022**, *534* (5), 2100382. https://doi.org/10.1002/andp.202100382.

(30) Baranov, P. G.; Orlinskii, S. B.; de Mello Donegá, C.; Schmidt, J. High-Frequency EPR and ENDOR Spectroscopy on Semiconductor Quantum Dots. *Appl. Magn. Reson.* **2010**, *39* (1), 151–183. https://doi.org/10.1007/s00723-010-0151-y.

(31) Gupta, J. A.; Awschalom, D. D.; Peng, X.; Alivisatos, A. P. Spin Coherence in Semiconductor Quantum Dots. *Phys. Rev. B* **1999**, *59* (16), R10421–R10424. https://doi.org/10.1103/PhysRevB.59.R10421.

(32) Siebers, B.; Biadala, L.; Yakovlev, D. R.; Rodina, A. V.; Aubert, T.; Hens, Z.; Bayer, M. Exciton Spin Dynamics and Photoluminescence Polarization of CdSe/CdS Dot-in-Rod Nanocrystals in High Magnetic Fields. *Phys. Rev. B* **2015**, *91* (15), 155304. https://doi.org/10.1103/PhysRevB.91.155304.

(33) Hu, R.; Yakovlev, D. R.; Liang, P.; Qiang, G.; Chen, C.; Jia, T.; Sun, Z.; Bayer, M.; Feng, D. Origin of Two Larmor Frequencies in the Coherent Spin Dynamics of Colloidal CdSe Quantum Dots Revealed by Controlled Charging. *J. Phys. Chem. Lett.* **2019**, *10* (13), 3681–3687. https://doi.org/10.1021/acs.jpclett.9b01534.

(34) DiVincenzo, D. P. The Physical Implementation of Quantum Computation. *Fortschritte Phys.* **2000**, *48* (9–11), 771–783. https://doi.org/10.1002/1521-3978(200009)48:9/11<771::AID-PROP771>3.0.CO;2-E.

(35) Liu, W. K.; Whitaker, K. M.; Smith, A. L.; Kittilstved, K. R.; Robinson, B. H.; Gamelin, D. R. Room-Temperature Electron Spin Dynamics in Free-Standing ZnO Quantum Dots. *Phys. Rev. Lett.* **2007**, *98* (18), 186804. https://doi.org/10.1103/PhysRevLett.98.186804.

(36) Whitaker, K. M.; Ochsenbein, S. T.; Smith, A. L.; Echodu, D. C.; Robinson, B. H.; Gamelin, D. R. Hyperfine Coupling in Colloidal N-Type ZnO Quantum Dots: Effects on Electron Spin Relaxation. *J. Phys. Chem. C* **2010**, *114* (34), 14467–14472. https://doi.org/10.1021/jp106356y.

(37) Kim, J.; Wong, C. Y.; Scholes, G. D. Exciton Fine Structure and Spin Relaxation in Semiconductor Colloidal Quantum Dots. *Acc. Chem. Res.* **2009**, *42* (8), 1037–1046. https://doi.org/10.1021/ar8002046.

(38) Ma, H.; Jin, Z.; Zhang, Z.; Li, G.; Ma, G. Exciton Spin Relaxation in Colloidal CdSe Quantum Dots at Room Temperature. *J. Phys. Chem. A* **2012**, *116* (9), 2018–2023. https://doi.org/10.1021/jp2116643.

(39) Olshansky, J. H.; Harvey, S. M.; Pennel, M. L.; Krzyaniak, M. D.; Schaller, R. D.; Wasielewski, M. R. Using Photoexcited Core/Shell Quantum Dots To Spin Polarize Appended Radical Qubits. *J. Am. Chem. Soc.* **2020**, *142* (31), 13590–13597. https://doi.org/10.1021/jacs.0c06073.

(40) Wang, J.; Ding, T.; Nie, C.; Wang, M.; Zhou, P.; Wu, K. Spin-Controlled Charge-Recombination Pathways across the Inorganic/Organic Interface. *J. Am. Chem. Soc.* **2020**, *142* (10), 4723–4731. https://doi.org/10.1021/jacs.9b12724.

(41) Weinberg, D. J.; Dyar, S. M.; Khademi, Z.; Malicki, M.; Marder, S. R.; Wasielewski, M. R.; Weiss, E. A. Spin-Selective Charge Recombination in Complexes of CdS Quantum Dots and Organic Hole Acceptors. *J. Am. Chem. Soc.* **2014**, *136* (41), 14513–14518. https://doi.org/10.1021/ja507301d.

(42) Jin, T.; Uhlikova, N.; Xu, Z.; Zhu, Y.; Huang, Y.; Egap, E.; Lian, T. Enhanced Triplet State Generation through Radical Pair Intermediates in BODIPY-Quantum Dot Complexes. *J. Chem. Phys.* **2019**, *151* (24), 241101. https://doi.org/10.1063/1.5136045.
(43) Liu, W. K.; Whitaker, K. M.; Kittilstved, K. R.; Gamelin, D. R. Stable Photogenerated Carriers in Magnetic Semiconductor Nanocrystals. *J. Am. Chem. Soc.* **2006**, *128* (12), 3910–3911. https://doi.org/10.1021/ja060488p.
(44) Germeau, A.; Roest, A. L.; Vanmaekelbergh, D.; Allan, G.; Delerue, C.; Meulenkamp, E. A. Optical Transitions in Artificial Few-Electron Atoms Strongly Confined inside ZnO Nanocrystals. *Phys. Rev. Lett.* **2003**, *90* (9), 097401. https://doi.org/10.1103/PhysRevLett.90.097401.
(45) Kim, J. Y.; Kim, Y. H.; Kim, Y. S. Indoline Dyes with Various Acceptors for Dye-Sensitized Solar Cells. *Curr. Appl. Phys.* **2011**, *11* (1), S117–S121. https://doi.org/10.1016/j.cap.2010.11.098.
(46) Anta, J. A.; Guillén, E.; Tena-Zaera, R. ZnO-Based Dye-Sensitized Solar Cells. *J. Phys. Chem. C* **2012**, *116* (21), 11413–11425. https://doi.org/10.1021/jp3010025.
(47) Matsui, M.; Kotani, M.; Kubota, Y.; Funabiki, K.; Jin, J.; Yoshida, T.; Higashijima, S.; Miura, H. Comparison of Performance between Benzoindoline and Indoline Dyes in Zinc Oxide Dye-Sensitized Solar Cell. *Dyes Pigments* **2011**, *91* (2), 145–152. https://doi.org/10.1016/j.dyepig.2011.02.009.
(48) Guerin, V. M.; Magne, C.; Pauporté, Th.; Le Bahers, T.; Rathousky, J. Electrodeposited Nanoporous versus Nanoparticulate ZnO Films of Similar Roughness for Dye-Sensitized Solar Cell Applications. *ACS Appl. Mater. Interfaces* **2010**, *2* (12), 3677–3685. https://doi.org/10.1021/am1008248.
(49) Meulenkamp, E. A. Synthesis and Growth of ZnO Nanoparticles. *J. Phys. Chem. B* **1998**, *102* (29), 5566–5572. https://doi.org/10.1021/jp980730h.
(50) Lommens, P.; Lambert, K.; Loncke, F.; De Muynck, D.; Balkan, T.; Vanhaecke, F.; Vrielinck, H.; Callens, F.; Hens, Z. The Growth of Co:ZnO/ZnO Core/Shell Colloidal Quantum Dots: Changes in Nanocrystal Size, Concentration and Dopant Coordination. *ChemPhysChem* **2008**, *9* (3), 484–491. https://doi.org/10.1002/cphc.200700753.
(51) Cappel, U. B.; Moia, D.; Bruno, A.; Vaissier, V.; Haque, S. A.; Barnes, P. R. F. Evidence for Photo-Induced Charge Separation between Dye Molecules Adsorbed to Aluminium Oxide Surfaces. *Sci. Rep.* **2016**, *6* (1), 21276. https://doi.org/10.1038/srep21276.
(52) Buckley, C. D.; Hunter, D. A.; Hore, P. J.; McLauchlan, K. A. Electron Spin Resonance of Spin-Correlated Radical Pairs. *Chem. Phys. Lett.* **1987**, *135* (3), 307–312. https://doi.org/10.1016/0009-2614(87)85162-X.
(53) Kobori, Y.; Fuki, M.; Murai, H. Electron Spin Polarization Transfer to the Charge-Separated State from Locally Excited Triplet Configuration: Theory and Its Application to Characterization of Geometry and Electronic Coupling in the Electron Donor−Acceptor System. *J. Phys. Chem. B* **2010**, *114* (45), 14621–14630. https://doi.org/10.1021/jp102330a.
(54) Weber, S.; Biskup, T.; Okafuji, A.; Marino, A. R.; Berthold, T.; Link, G.; Hitomi, K.; Getzoff, E. D.; Schleicher, E.; Norris, J. R. Origin of Light-Induced Spin-Correlated Radical Pairs in Cryptochrome. *J. Phys. Chem. B* **2010**, *114* (45), 14745–14754. https://doi.org/10.1021/jp103401u.
(55) Weber, S. Transient EPR. In *EPR Spectroscopy: Fundamentals and Methods*; John Wiley & Sons Ltd, 2018.
(56) Stehlik, D.; Bock, C. H.; Petersen, J. Anisotropic Electron Spin Polarization of Correlated Spin Pairs in Photosynthetic Reaction Centers. *J. Phys. Chem.* **1989**, *93* (4), 1612–1619. https://doi.org/10.1021/j100341a084.
(57) Hore, P. J. Analysis of Polarized EPR Spectra. In *Advanced EPR: Applications in biology and biochemistry*; Elsevier: Amsterdam, 1989; pp 405–440.

Table of Contents artwork